

# Self-Organization of Fast Ions and Toroidicity-Induced Alfvén Eigenmodes

TODO Yasushi and SATO Tetsuya

*Theory and Computer Simulation Center*

*National Institute for Fusion Science, Toki 509-5292, Japan*

(Received: 25 December 1998 / Accepted: 1 July 1999)

## Abstract

Nonlinear evolution of the fast ions and the toroidicity-induced Alfvén eigenmodes (TAEs) has been investigated with the Fokker-Planck-magnetohydrodynamic simulation. Source and slowing-down of fast ions are considered in the Fokker-Planck equation. It is found that the TAEs reach steady saturation levels for a slowing-down time comparable to the damping time. TAE bursts take place when the slowing-down time is much longer than the damping time of the TAEs and the fast-ion pressure is sufficiently high. The fast-ion distribution is globally flattened when the TAE bursts take place.

## Keywords:

TAE, fast-ion source, slowing down, steady state, burst

## 1. Introduction

The toroidicity-induced Alfvén eigenmode (TAE) is a shear-Alfvén eigenmode in toroidal plasmas [1]. Nonlinear evolution of TAEs is an important issue for fusion reactors, since TAEs with sufficiently large amplitude can induce fast-ion losses [2,3]. In the neutral-beam-injection heating experiments [2,4] TAEs show a recurrent bursting behavior. In the ion-cyclotron-range-of-frequency heating experiments [5,6] and D-T fusion experiments at TFTR [7], TAEs persist longer than the typical damping time.

Berk and Breizman [8] pointed out the significance of the distribution-forming-processes such as particle source, slowing down, pitch-angle scattering, and wave heating. They and their collaborators carried out one-dimensional particle simulations for a bump-on-tail instability with particle source and annihilation [9]. They showed that an isolated single mode with a sufficiently large annihilation rate has a steady saturation level and multiple overlapped modes with a small annihilation rate show a pulsating behavior.

Their work gave us a sufficient motivation to develop a comprehensive simulation code where the distribution-forming-processes are incorporated. As the first step towards such a comprehensive simulation of TAEs, we have developed a Fokker-Planck-magnetohydrodynamic (MHD) simulation code by incorporating particle source and slowing down for fast ions into the Vlasov-MHD simulation code [10]. Time evolution of the fast-ion distribution function in a four-dimensional phase space (three-dimensional real space and one-dimensional velocity space for the parallel velocity) is followed by a finite difference method. The pitch-angle scattering and wave heating are not considered in this work. In this paper, the simulation model is described in section 2 and the results of two typical cases are reported in section 3. Section 4 is devoted to summary.

## 2. Model

A kinetic-MHD hybrid model, which was used in

---

Corresponding author's e-mail: [todo@nifs.ac.jp](mailto:todo@nifs.ac.jp)

the Vlasov-MHD and particle-MHD simulations [10,11], is employed. In this model plasma is divided into two parts, namely, the background plasma and fast ions. The background plasma is described by the MHD equations and the electromagnetic field is given by the MHD description. This approximation is reasonable under the condition that the fast-ion density is much less than the background plasma density. The MHD equations are,

$$\frac{\partial \rho}{\partial t} = -\nabla \cdot (\rho \mathbf{v}), \quad (1)$$

$$\rho \frac{\partial}{\partial t} \mathbf{v} + \rho \mathbf{v} \cdot \nabla \mathbf{v} = -\nabla p + \frac{1}{\mu_0} (\nabla \times \mathbf{B}) \times \mathbf{B} + \nu \rho \Delta \mathbf{v}, \quad (2)$$

$$\frac{\partial \mathbf{B}}{\partial t} = -\nabla \times \mathbf{E}, \quad (3)$$

$$\frac{\partial p}{\partial t} = -\nabla \cdot (\rho \mathbf{v}) - (\gamma - 1) p \nabla \cdot \mathbf{v}, \quad (4)$$

$$\mathbf{E} = -\mathbf{v} \times \mathbf{B}, \quad (5)$$

where  $\mu_0$  is the vacuum magnetic permeability and  $\gamma$  is the adiabatic constant, and all the other quantities are conventional.

We consider a four-dimensional phase space  $(R, \varphi, z, v)$ , where  $v$  is the parallel velocity and  $(R, \varphi, z)$  are the cylindrical coordinates. We consider only the parallel velocity component for simplicity. We, however, adopt a Jacobian for the three-dimensional velocity space to be consistent with the slowing-down term. The equation for the distribution function of fast-ions is

$$\begin{aligned} \frac{\partial}{\partial t} f = & -\nabla \cdot (\mathbf{v}_D) - \frac{\partial}{\partial v} v^2 a_H f \\ & + C \frac{\partial}{\partial v} \left[ 1 + \left( \frac{v^3}{v_{\text{crit}}^3} \right) \right] f + \frac{S(\mathbf{x})}{v^2} \delta(v - v_0), \end{aligned} \quad (6)$$

$$\mathbf{v}_D = \frac{v}{B} \left[ \mathbf{B} + \frac{m_f}{q_f} v \nabla \times \mathbf{b} \right] + \frac{1}{B} [\mathbf{E} \times \mathbf{b}], \quad (7)$$

$$\mathbf{b} = \mathbf{B} / B, \quad (8)$$

$$a_H = \frac{v}{B} \nabla \times \mathbf{b} \cdot \mathbf{E}, \quad (9)$$

$$S(\mathbf{x}) = S_0 \exp[-(\alpha r)^2], \quad (10)$$

where  $v_{\text{crit}}$  is the critical velocity and  $v_0$  is the birth velocity of fast ions, and they are chosen to be equal to  $0.3v_A$  and  $1.5v_A$ , respectively. On the right-hand-side of Eq. (6), the third term and the fourth term represent the slowing down and the source of fast ions, respectively. In Eq. (10),  $\alpha$  is chosen to be equal to  $1/0.4a$ , where  $a$  is the minor radius.

When the first and second terms on the right-hand-side of Eq. (6) are absent and  $v_{\text{crit}}$  is much smaller than  $v_0$ , steady fast-ion pressure at the magnetic axis is given by

$$P_0 = \frac{1}{2} m_f v_0^2 v_{\text{crit}}^3 S_0 / C. \quad (11)$$

We introduce the slowing-down time  $\tau_s$ , which is defined as

$$\tau_s = P_0 / m_f v_0^2 S_0. \quad (12)$$

The parameters  $C$  and  $S_0$  can be expressed through  $\tau_s$  and  $P_0$  as

$$C = \frac{1}{2} v_{\text{crit}}^3 / \tau_s, \quad (13)$$

and

$$S_0 = P_0 / m_f v_0^2 \tau_s, \quad (14)$$

The effect of fast ions on the MHD fluid is taken into account in the MHD momentum equation [10,11] and is given for the present case by

$$\begin{aligned} \rho \frac{\partial}{\partial t} \mathbf{v} + \rho \mathbf{v} \cdot \nabla \mathbf{v} = & \left( \frac{1}{\mu_0} \nabla \times \mathbf{B} - \mathbf{j}'_f \right) \times \mathbf{B} - \nabla p \\ & + \nu \rho \Delta \mathbf{v}, \end{aligned} \quad (15)$$

$$\mathbf{j}'_f = \mathbf{j}_{f\parallel} + \frac{1}{B} P \nabla \times \mathbf{b}, \quad (16)$$

where  $P$  is the fast-ion parallel pressure.

The initial condition is an MHD equilibrium where the aspect ratio is 3. The  $q$ -profile is shown in Fig. 1 with the radial profile of the source. We define the unit of length as the Larmor radius of a fast ion with the Alfvén velocity ( $\equiv v_A m_i / q_f B$ ) at the initial magnetic axis. The simulation domain is  $(32 \leq R \leq 64, 0 \leq z \leq 32)$ . The major radius of the initial magnetic axis ( $\equiv R_0$ )

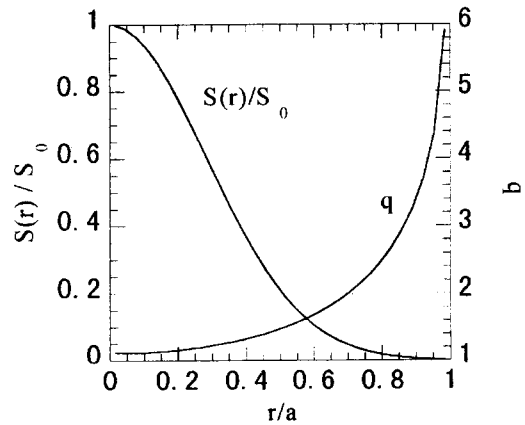


Fig. 1 The  $q$ -profile and the profile of the fast-ion source as a function of the minor radius.

is 50.5. We also define the unit of time as the Alfvén time ( $\tau_A \equiv R_0/v_A$ ). The system can be specified by three parameters  $\tau_s$ ,  $P_0$ , and  $v$ . In this paper a finite viscosity  $\nu = 2 \times 10^{-5} v_A R_0$  is considered to damp TAEs. It yields, for example, an  $e$ -folding damping time of  $130\tau_A$  for an  $n = 2$  TAE which is the most unstable TAE in the simulations described below. The Fokker-Planck equation for fast-ion and the full magnetohydrodynamic equations are solved by a finite difference method of a fourth-order accuracy in space and time.

### 3. Results

#### 3.1 $P_0 = 2\%$ (Normalized by the Magnetic Pressure) and $\tau_s = 100\tau_A$

In this case the slowing-down time is comparable to the damping time. TAEs with the toroidal mode numbers of 1, 2, and 3 are destabilized. The linear growth rates of  $n = 2$  and 3 TAEs are  $3.1 \times 10^{-2}\tau_A^{-1}$  and  $4.0 \times 10^{-2}\tau_A^{-1}$ , respectively. The  $n = 1$  TAE begins to grow at  $t = 270\tau_A$  with a growth rate of  $1.9 \times 10^{-3}\tau_A^{-1}$ . This delayed growth may be caused by some nonlinear effects due to the advanced growth of  $n = 2$  and 3 TAEs. Another Alfvén eigenmode is also destabilized with the toroidal mode number of 4 and with a roughly doubled frequency. In Fig. 2 shown is the time history of the radial magnetic fluctuations ( $\delta B_r$ ) with  $m/n = 2/1, 3/2, 4/3, 6/4$ , where  $m$  and  $n$  are the poloidal and toroidal mode numbers in a flux coordinate system ( $r, \theta, \varphi$ ), respectively. The  $n = 2-4$  eigenmodes are localized in the core region, where the fast-ion source and its spatial gradient are sufficient to destabilize them. It can be seen that  $n = 2-4$  modes reach roughly steady saturation levels after  $t = 500\tau_A$ . The fast-ion distribution averaged in the toroidal angle with  $v = v_A$  and  $t = 900\tau_A$  is shown in Fig. 3. The distribution is similar to the fast-ion source profile in Fig. 1, but is locally flattened in the core region where the TAE activity is strong.

#### 3.2 $P_0 = 4\%$ and $\tau_s = 1000\tau_A$

In this case the slowing-down time is much longer than the damping time and the fast-ion pressure is relatively high. TAEs with toroidal mode numbers from 1 to 4 are destabilized. The  $n = 1$  and 2 TAEs are the same as those described in section 3.1. On the other hand, the  $n = 3$  and 4 eigenmodes are different. They are TAEs, and spatially peak at outer locations. Time history of the radial magnetic fluctuations ( $\delta B_r$ ) with  $m/n = 2/1, 3/2, 4/3$ , and  $6/4$  is shown in Fig. 4. It can be seen that TAE bursts take place three times. At the first burst, the most unstable  $n = 2$  TAE is destabilized first.

Later than this precursory growth of the  $n = 2$  TAE, the other TAEs grow to levels comparable to that of the  $n = 2$  TAE. At the second and third bursts, all of the TAEs behave coherently.

The fast-ion distribution averaged in the toroidal angle with  $v = v_A$  and  $t = 2800\tau_A$  is shown in Fig. 5. The fast-ion distribution is globally flattened compared to the fast-ion source profile in Fig. 1. This indicates

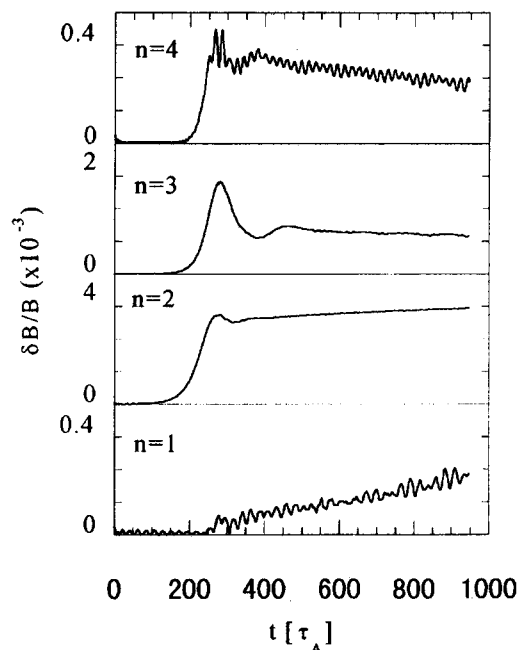


Fig. 2 Time history of the radial magnetic fluctuation ( $\delta B_r$ ) with  $m/n = 2/1, 3/2, 4/3, 6/4$  for  $P_0 = 2\%$  and  $\tau_s = 100\tau_A$ .

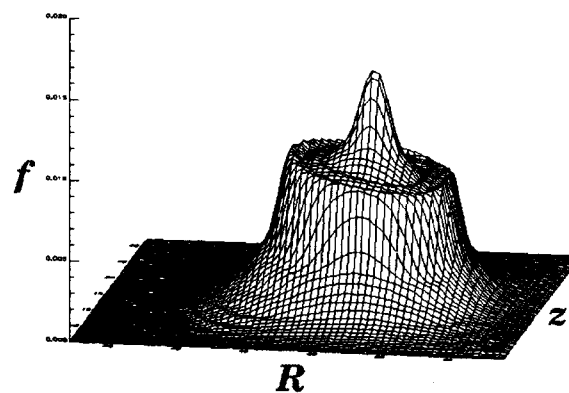


Fig. 3 Fast ion distribution as a function of  $R$  and  $z$ , averaged in the toroidal angle with  $v = v_A$  for  $P_0 = 2\%$  and  $\tau_s = 100\tau_A$  at  $t = 900\tau_A$ .

that the fast-ion distribution is significantly affected by TAEs. The TAE bursts are considered to be a self-organization resulting from a cycle of reformation of fast-ion distribution, growth of TAEs due to increasing fast-ion drive, global flattening of fast-ion distribution, and damping of TAEs due to reduced fast-ion drive. The detail of this cycle will be discussed elsewhere, since it is beyond the scope of a brief paper.

**4. Summary**

In this paper we have investigated the nonlinear evolution of fast ions and the TAEs with the source and the slowing-down terms in the Fokker-Planck equation. We have demonstrated that the consideration of the distribution-forming-processes of fast ions is crucial to understand the time evolution of TAEs and fast ions.

Simulation results are summarized as follows:

1. When the time scale of the distribution-forming-process [the slowing-down time in this work] is comparable to the damping time, TAEs persist after saturation with steady amplitudes.
2. When the time scale of the distribution-forming-process is longer than the damping time and the fast-ion pressure is sufficiently high, TAE bursts take place and the fast-ion distribution is globally flattened.

**Acknowledgments**

The authors would like to express their thanks to all members of the Complexity Simulation Group for useful discussions. Numerical computations were performed at the Advanced Computing System for Complexity Simulation of National Institute for Fusion Science.

**References**

[1] C.Z. Cheng and M. S. Chance, *Phys. Fluids* **29**, 3659 (1986).  
 [2] H.H. Duong *et al.*, *Nucl. Fusion* **33**, 749 (1993).  
 [3] D.S. Darrow *et al.*, *Nucl. Fusion* **37**, 939 (1997).  
 [4] K.L. Wong *et al.*, *Phys. Rev. Lett.* **66**, 1874 (1991).  
 [5] K.L. Wong *et al.*, *Plasma Phys. Control. Fusion* **36**, 879 (1994).  
 [6] H. Kimura *et al.*, *J. Plasma Fusion Res.* **71**, 1147 (1995).  
 [7] R. Nazikian *et al.*, *Phys. Rev. Lett.* **78**, 2976 (1997).  
 [8] H.L. Berk and B.N. Breizman, *Phys. Fluids* **B 2**,

2226, 2235, 2246 (1990).  
 [9] H.L. Berk, B.N. Breizman and M. Pekker, *Phys. Plasmas* **2**, 3007 (1995).  
 [10] Y. Todo *et al.*, *Phys. Plasmas* **2**, 2711 (1995).  
 [11] Y. Todo and T. Sato, *Phys. Plasmas* **5**, 1321 (1998).

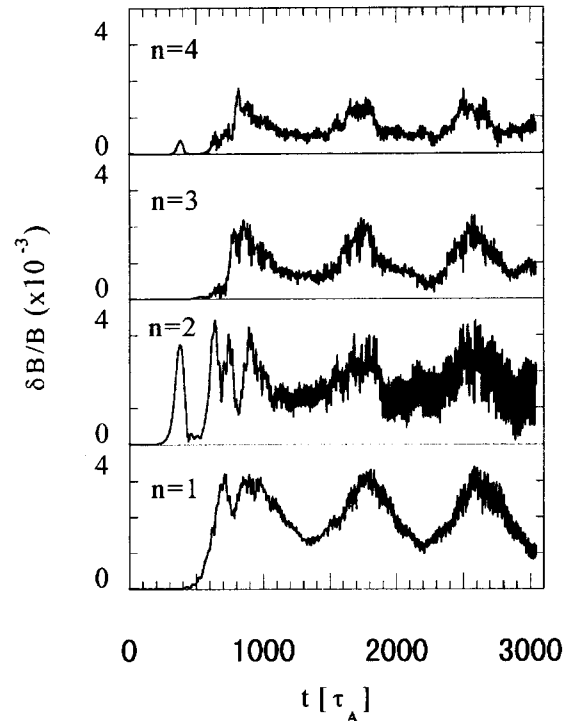


Fig. 4 Time history of the radial magnetic fluctuation ( $\delta B_r$ ) with  $m/n = 2/1, 3/2, 4/3, 6/4$  for  $P_0 = 4\%$  and  $\tau_s = 1000\tau_A$ .

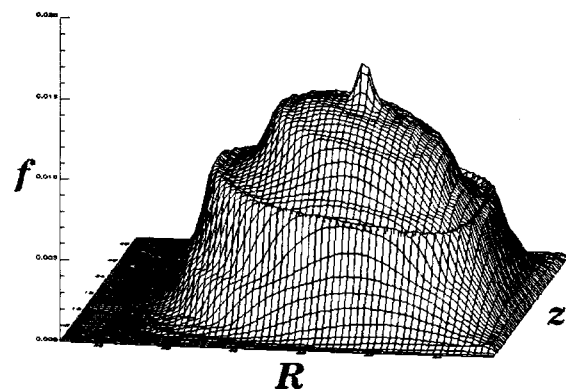


Fig. 5 Fast ion distribution as a function of R and z, averaged in the toroidal angle with  $v = v_A$  for  $P_0 = 4\%$  and  $\tau_s = 1000\tau_A$  at  $t = 2800\tau_A$ .